Numerical Analysis of Three-Dimensional Elastic Membrane Wings

P. S. Jackson*
University of Auckland, Auckland, New Zealand
and
G. W. Christie†
Systems Science and Research, Auckland, New Zealand

This paper presents a numerical method for predicting the behavior of an elastic membrane wing under aerodynamic loading. A method for finding the pressure distribution generated by flow over a given three-dimensional surface is combined with another for finding the shape of a given membrane under a given pressure distribution. The pressure is calculated using a vortex lattice simulation of potential flow, and the shape is determined using a finite element representation of the membrane. An iterative scheme is employed to solve the resulting nonlinear equations which relate the shape and loading to the displacements of the surface. A simple example is given, in which the lift and stress distribution are calculated for a membrane wing with the shape and boundary constraints of an idealized hang glider. The method is equally applicable to yacht sails.

I. Introduction

THE pressure distribution acting on a lifting surface is determined by its shape, and in most aerodynamic applications this shape is fixed—that is, the aerodynamic loads do not themselves cause significant changes in the shape of the lifting surface. However, this is not the case when the lifting surface is an elastic membrane, as in sails and hang-gliders, since the twist and camber of such wings under load may be quite different from their unloaded values. As the shape determines the pressure, but the pressure is in turn determined by the shape, predicting the shape from first principles requires the simultaneous solution of the aerodynamic and structural problems. This paper describes a numerical model for elastic membrane wings that predicts wing shapes, strains, and stresses and the corresponding coefficients of lift and induced drag.

The two-dimensional problem for a flexible membrane between fixed leading and trailing edges was originally studied by Thwaites[1] and Nielsen,[2] and Newman[3] has reviewed more recent work on this subject. The stress in the membrane (that is, the tension per unit width) emerges as part of the solution. When the membrane is elastic, the solution is no more difficult, in principle (since the surface has the same shape and tension), as an inextensible sail of the same length under load.

The three-dimensional problem is much more complicated. The initial shape must now be specified in detail; the chord length, twist, maximum camber and section shape may all vary along the span. Although there are slightly fewer variables when the initial shape is developable, this situation is not usual. In addition, the nature of the edge restraints must be given around the boundary of the membrane—each edge can be free, fixed, or restrained to slide in a particular direction (as along a mast track in the case of a yacht sail), or may have specified edge force or displacement. A particularly awkward condition arises for an edge that is free to slide along a cable which is itself deformable (like the forestay of a yacht). The membrane thickness and its elastic constants are also required for every part of the surface. At least the elastic modulus E and Poisson's ratio must be given, but commonly used fabrics are more or less anisotropic (modern composites being up to ten times stiffer in one direction than in another) and require still more elastic constants. Finally, both the angle and speed of the incident flow may vary along the span (as in sailing).

The elastic stiffness of the membrane is measured by Ed, where d is the membrane thickness. Dimensional analysis can then be used to reduce the number of variables. The elastic stiffness relative to the applied load is expressed by the parameter $Æ = Ed/qc$, where q is the incident stagnation pressure and c the reference length of the planform (here the maximum chord length). This number does not appear to have any consistent name in the literature, so we shall refer to it here as the "aeroelastic number." Its physical significance is that two membrane wings of different size but with the same value of $Æ$ and the same initial shape and boundary conditions will develop the same lift coefficient and strain distribution at the same angle of attack, that is, they will develop the same final shape. This presumes that the Reynolds number is unimportant, and the reasons for this are made below. All the other variables mentioned above are already nondimensional, and none can be presumed to be unimportant.

Given the complexity of the three-dimensional problem it is not surprising that earlier workers have only studied wing configurations which have some simplifying feature. Nielsen et al.[4] analyzed a low aspect ratio parawing using slender body theory; in transverse sections both the flow and the membrane structure were assumed to behave as if two-dimensional. Sneyd et al.[5] examined an inelastic triangular membrane supported by a leading edge spar and an elastic trailing edge cable, taking the membrane to behave as if two-dimensional in chordwise sections but causing three-dimensional deflections of the cable. Ormiston[6] carried out a similar analysis of a rectangular membrane with trailing edge cable. He assumed that the spanwise structural behavior of the membrane was independent of its chordwise action (zero Poisson's ratio), and that the aerodynamics was two-dimensional. Holla et al.[7] developed a method for a rec-

Received Feb. 7, 1986; revision received June 27, 1986.

*Professor, Department of Mechanical Engineering.
†Director.

tangular membrane that was fully restrained at the edges and with a high level of prestress, the membrane then being assumed to remain in this state of uniform biaxial tension under aerodynamic loading. No model seems to apply the assumption of small displacements consistently to both the aerodynamic and structural problems. Generally the assumptions made for the structural problem are the stronger, reflecting the fact that flat membranes have a highly nonlinear response to any transverse load.

Several authors have neglected the flexible behavior of the membrane entirely in order to study the aerodynamics of the interaction between two sails in close proximity. The classic work in this area was performed by Milgram[8] who first produced a design method for yacht sails, and subsequently[9] carried out a systematic study of the effects of planform on performance. He used lifting line theory to optimize span loading, and an assumed chordwise pressure distribution together with a linearized vortex lattice to obtain the required sail shapes. However, this method did not show whether a membrane shape so obtained could actually be in equilibrium under the action of its associated pressure distribution. There is also the question of how well a two-dimensional lattice can represent overlapping surfaces, especially in the area of overlap. Both Thrasher et al.[10] and Register[11] used three-dimensional lattices to study this problem, but used direct methods for analyzing the aerodynamic performance of given (rigid) shapes.

A fully numerical method for three-dimensional lifting membranes was introduced by Jackson.[12] His approach was to find the pressure distribution acting on the initial shape, and then find the shape the membrane would take up under the action of this (fixed) pressure. This process was then repeated until a stable shape was obtained. The pressure distribution was found using a vortex-lattice method, and the shape with a finite-element model developed by Christie.[13] The iteration method was rather clumsy but it did show that the procedure could be made to converge, and thus led to the much more efficient method described below. Some particular applications of the method to the analysis of yacht sails have been described elsewhere.[14]

II. The Solution Method

Outline

It is assumed that the initial geometry, boundary conditions, and material properties of a membrane wing have been specified. The problem is to find the final shape of the wing when placed in a given airstream at a particular angle of attack. The solution method described here is based on the finite-element formulation for large strain plane-stress problems devised by Oden and Sato,[15] with the addition of a vortex-lattice method for predicting surface pressures. The method is an iterative one, in which at each step the membrane shape is adjusted toward an equilibrium position using the pressure distribution calculated for the current shape. The continuous membrane surface is approximated by an assembly of triangular elements. The equations of equilibrium are expressed in terms of the unknown positions of the nodes and then solved for the nodal displacements required to achieve equilibrium. As few readers will be familiar with both the finite-element and vortex-lattice methods, a short description of each is given subsequently.

Elastic and Nodal Forces

First, it is necessary to find a relationship between the displacements of the nodes of a single element and the consequent nodal forces generated by internal strains. The analysis is greatly simplified by using triangular elements with displacements that vary linearly on the element surface; the initially plane elements therefore remain plane. Within a particular element the three components of displacement, y_i ($i=1,2,3$), can be written as a rigid-body motion plus a component for the distortion of the element. As this expression must be satisfied by the displacement u_{Ni} of each of the N ($N=1,2,3$) corner nodes, it can be rewritten in terms of these nodal displacements; that is

$$y_i = k_N u_{Ni} + c_{N\beta} u_{Ni} x_\beta \tag{1}$$

where x_β ($\beta=1,2$) are the local coordinates in the plane of the element. [Note that repeated indices in Eq. (1) imply summation over the dimensions of the index]. Expressions for the transformation matrices k_N and c_{Ni} are given by Oden and Sato,[15] but the essential feature is that as the formulation is Lagrangian, the matrices depend only on the *initial* geometry of the element, and therefore need be calculated only once. They also enable Green's strain tensor in the plane of the element to be expressed in terms of the nodal displacements

$$\gamma_{\alpha\beta} = \frac{1}{2}\left[\frac{\partial u_\alpha}{\partial x_\beta} + \frac{\partial u_\beta}{\partial x_\alpha} + \frac{\partial u_m}{\partial x_\alpha}\cdot\frac{\partial u_m}{\partial x_\beta}\right]$$

$$= \frac{1}{2}(c_{N\alpha} u_{N\beta} + c_{N\beta} u_{N\alpha} + \ldots) \tag{2}$$

Whereas the solution method here is actually formulated for large strains, the strains which occur in practice are numerically small (although large by engineering standards, they are generally less than 1%) and therefore the nonlinear term in the strain definition has been dropped. This does not imply that the displacements are also small. There are no shear strains on planes within the element ($\gamma_{\alpha 3}=0$), and the strain normal to the element merely measures its change in thickness.

It is now necessary to find the forces f_{Ni} at each node N which are generated by arbitrary displacements y_i. A common way of specifying the constitutive relation is to work in terms of the strain energy function, as this readily accommodates materials with a nonlinear stress/strain response. However, the equations described herein are only for a linear Hookean material as these are relatively familiar to most engineers. The constitutive law for a general Hookean material gives the relationship between stress and strain as

$$\sigma_{ij} = C_{ijkl}\gamma_{kl} \tag{3}$$

where C is the fourth-order elasticity tensor (in a form appropriate to plane stress). For isotropic materials, C has just two independent components, and Eq. (3) reduces to its usual plane stress form involving the elastic modulus E and Poisson's ratio ν. For orthotropic materials in plane stress the C sensor has six independent components form (see, for example, Hearman[16]). For all materials the constitutive law must be modified so that the membrane is unable to withstand compressive stress, as the physical response in this case is the appearance of wrinkles. Thus if a compressive principal stress is detected, the appropriate form of Eq. (3) is for uniaxial rather than biaxial plane stress.

Finally, if node N is given an arbitrary displacement Δy_{Nk} from its equilibrium position, then the principle of virtual work gives the work done by the nodal force f_{Nk} at N as $f_{Nk}\Delta y_{Nk} = \int \sigma_{\alpha\beta}\Delta\gamma_{\alpha\beta}\,dv$ where $\Delta\gamma$ is the additional strain due to the displacement (see Fung[17]). The integral is over the element volume v, so terms within it are constant for the constant-strain elements. Since the expression holds for arbitrary Δy, it reduces to $f_{Nk} = \sigma_{\alpha\beta}(\partial\gamma_{\alpha\beta}/\partial y_{Nk})v$ (repeated indices implying summation). Using Eq. (2) this becomes

$$f_{Nk} = \sigma_{\alpha\beta}\tfrac{1}{2}(C_{N\alpha}\delta_{k\beta} + C_{N\beta}\delta_{k\alpha})v$$

$$= \sigma_{\alpha k} C_{N\alpha} v \tag{4}$$

(where δ_{ij} is the Kronecker delta function). If this is combined with Eqs. (2) and (3), the desired relationship between the nodal displacements is obtained. The displacements must now be found such that the nodal forces are in equilibrium with externally applied forces, namely those due to pressure.

Pressure Prediction

Numerous so-called "panel" methods are available for calculating the pressure generated by inviscid flow around a lifting body of known shape. In principle these methods are all equivalent, however in practice they require significantly different levels of programming and computational effort. The main purpose of this paper is to describe a method of computing flows around membrane wings; the exact technique used for the pressure computation is not of central importance, therefore a simple vortex-lattice method has been adopted.

The pressure force acting on each element is calculated using inviscid-flow theory in which the lifting surface is replaced by a vortex sheet lying on the surface of the wing and its wake. Within each iteration for the wing shape the position of the vortex sheet is regarded as known, and the sheet strength w can be calculated. If the jump in velocity potential across the sheet is ϕ, the fact that w is orthogonal to the local unit normal of the surface n leads to

$$w = \nabla\phi x n \tag{5}$$

The doublet distribution ϕ must also be such that the boundary condition of no flow penetration through the lifting surface is satisfied. As the surface is already discretized into triangles, the solution is greatly simplified by assuming that ϕ and its associated induced velocity are constant over each triangle. This is equivalent to concentrating all the vorticity within each element into vortex lines around the triangular perimeter, forming a so-called "vortex lattice." Taking the divergence of Eq. (5) illustrates the Helmholtz requirement that w be nondivergent, and can be guaranteed by treating each element as forming a closed-vortex loop of strength Γ. The total velocity at any point is then the sum of the incident velocity V and the velocity induced there by the vortex loops, so that the no-penetration condition applied at one control point of element M becomes $(B_{MN}\Gamma_N + V_M)\cdot n_M = 0$, where the influence coefficient B is the velocity induced at the point M by the vortex loop encircling element N. Since B is a function only of the (known) element and wake geometry, an equation of this type can be formed for each element, and the resulting system of equations solved for the loop strengths Γ_N. The Kutta condition is enforced at the trailing edge by setting the strength of vortices aong the trailing edge to zero, so that loops on the trailing-edge elements extend into the wake and form a trailing vortex system.

Once the loop strengths Γ_N are known, those of the individual line vortices are given by the jumps in Γ between elements. The tangential velocity v induced at each control point can also be found using the influence functions B_{MN}. Since the pressure jump is assumed constant over each element, it can be found from the force induced in the surrounding vortex lines. (For vortices not on the wing boundary, the force is shared between neighboring elements.) If an element has area A and sides made up of vortex lines of length ℓ_i and strength Γ_i, the pressure jump would be

$$p = -[(V+v)\times w]\cdot n \qquad \text{where } w = \Sigma\ell_i\Gamma_i/2A$$

This expression for pressure can also be obtained using Bernoulli's equation, with w given by Eq. (5). On each element ϕ is constant in this formulation, but a local gradient of ϕ can be estimated from the jumps in ϕ (that is, the vortex strengths) that occur at the edges of the element. This argument also leads exactly to the expression given for w, from which the pressure jump is easily evaluated at each control point. In the case of yacht sails, the presence of the water surface is easily accounted for by including the image of every vortex loop in the surface, and the same device can be used for wings symmetric about a centerline. The vector sum of the pressure forces may now be assembled to give lift and induced drag. The leading- and side-edge forces are estimated by the forces induced on the line vortices along these edges (using their midpoint velocities). These are less significant in calculating the shape of membrane wings as such forces are usually transmitted to a spar or cable (if they occur at all in practice).

The usual formulation of the vortex-lattice method uses quadrilateral elements, with transverse vortices placed across the quarter-chord and the control point on the three-quarter-chord. The justification for this has its origins in the Weissinger approximation, and in James'[18] demonstration that in two-dimensional flow this arrangement leads to the correct form of leading-edge singularity as the number of chordwise elements increases. However, here the numerical advantages of having the vortex lines coincide with the finite-element boundaries are considerable, so the lattice is triangular instead. There is then no clear choice for control point location. Asfar et al.[19] argue that it should be placed at the point of minimum self-induced velocity. However here the finite-element formulation assumes a constant pressure over each element so that the pressure force can be replaced by equivalent forces of one-third magnitude acting at the corners. It therefore seems more appropriate to choose the element centroid as the control point, and this choice has been adopted herein.

The authors are aware that the use of a triangular lattice is unusual, but know of no reason (intrinsic to potential theory) for avoiding it. Its performance no doubt could be improved by trying different variations in element density, control points, and Kutta conditions, but this is beyond the scope of this paper. It would probably be more sensible to replace the vortex-lattice method by a more accurate method, but there would be little point in doing this without also upgrading the finite-element method.

There is also a problem regarding the position of the wake. The wake position is actually unknown, and should emerge as part of the solution (from the condition that it be force-free, so that vortex lines coincide with streamlines). However, the customary assumption is made that the wake extends from the trailing edge to downstream infinity in the direction of the incident flow. For a single lifting surface this approximation is reasonably good, as the actual wake position has only a weak effect on the results. However, as the

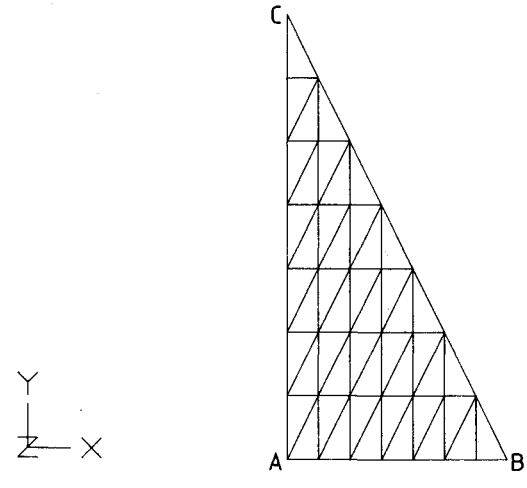

Fig. 1 Finite-element and vortex-lattice mesh for an initially plane triangular wing.

Table 1 Comparison of present method with classical vortice-lattice method,[15] for a delta wing

Lattice	$N \times M$	Lift slope, $C_{L\alpha}$	Induced drag, C_D/C_L^2
Triangular	4×8	0.0606	0.064
	6×10	0.0600	0.070
Quadrilateral	4×8	0.0609	0.070
	6×10	0.0607	0.071

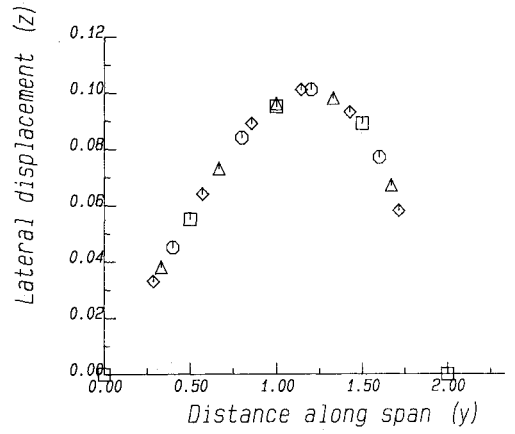

Fig. 2 Lateral displacement of trailing edge (side BC of Fig. 1); (number of elements: □, 16; ○, 25; △, 36; ◇, 49).

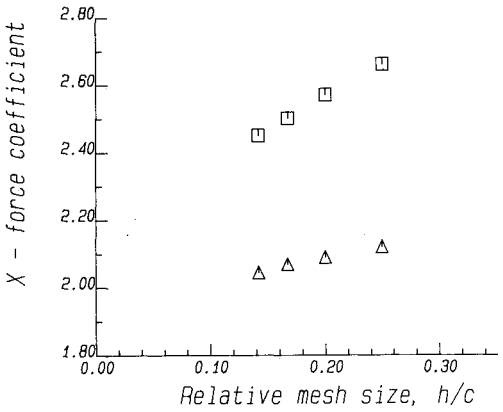

Fig. 3 Dependence of x component of restraining force at B (Fig. 1) on element size (△, uniform pressure; □, aerodynamic pressure).

wake is then not force-free the Kutta requirement of zero pressure jump at the trailing edge cannot be guaranteed and the calculated pressures near the trailing edge will be slightly in error. The proper treatment is to allow the wake to take up a force-free position, for which iterative methods are well established. When two surfaces interact (as the main and foresail of a yacht), the wake from the leading surface has a strong effect on the other surface so the correct implementation of force-free wakes is then essential.

The use of potential-flow theory naturally means that viscous drag is not accounted for, nor can separation be predicted. However, Newman and Goland[20] have given a simple argument for two-dimensional membranes which suggest that viscous stresses play a negligible part in the equilibrium of the membrane, and therefore do not affect the membrane shape. There is no reason to expect their effect on three-dimensional membranes to be any greater, so that the present method could be used to determine the external pressure gradient necessary for conventional boundary-layer computations over a wing of known shape.

The overall accuracy of the method was tested against a classical vortex-lattice method by Margason and Lamar.[21] The test shape was a plane swept wing having a leading-edge angle of 45 deg, a taper ratio of 0.0, and aspect ratio 4.5. The lattice array used was uniform and regular (in the sense of Fig. 1) with N elements along the center chord and M spanwise elements. Table 1 compares the results of the different methods. Margason and Lamar used a quadrilateral lattice, which for the same M and N has the same number of elements but an element density that is much higher at the wingtip. It appears that the triangular lattice converges less slowly as the element size decreases, but that its accuracy is quite sufficient for its present purpose. The slow convergence in drag is most likely due to the treatment of leading-edge suction; as noted above, the triangular lattice does not represent the leading-edge singularity as well as the classical quadrilateral layout with three-quarter-chord control point.

Membrane Equilibrium

The final step in assembling the equtions is to express the equilibrium between nodal elastic forces and pressure forces. Since the elastic forces are only available in coordinates local to each element, it is necessary to transform these to a global reference frame. The method of doing this is outlined by Oden and Sato[15]; we shall merely note that the transformation is itself a function of the unknown nodal displacements. The sum of the forces due to the strain in the elements attached to each node must balance the pressure forces there, so for each node there is an equation of the form

$$\Sigma(f_k - p_k) = 0 \tag{6}$$

where the sum is over the elements connected to the node. As both types of force depend nonlinearly on the nodal displacements, an iterative solution method is needed; the Newton-Raphson method is used as follows.

If the surface is perturbed by a small increment dy_m from an equilibrium surface Y_{om}, so that the new displacements are $Y_m = Y_{om} - dy_m$, then Eq. (6) can be approximated by the expansion

$$[f_k(Y_{om}) - p_k(Y_{om})] = 0$$

$$= [f_k(Y_m) - p_k(Y_m)] + dy_m J_{km} + \ldots$$

where

$$J_{km} = \frac{\partial f_k}{\partial y_m} - \frac{\partial p_k}{\partial y_m}$$

is the Jacobian matrix evaluated at Y_m. If all the other terms can be found then the equation can be solved for dy_m, thus providing an iterative procedure for proceeding from a current solution Y_m to an improved one. The first term on the right-hand side represents the unbalance in nodal forces for the current solution and can be calculated using the full nonlinear equations outlined in the preceding section. Both terms in the Jacobian can be estimated numerically. The first term represents the nodal stiffness and is obtained by calculating the change in nodal force which occurs when the node is displaced slightly from its current position while all other nodes are held fixed; this also uses the full equations for element stiffness. The second term represents a stiffness due to change in aerodynamic loading with position. If one node is similarly displaced normal to the surface, its change in pressure force will generally be in a direction tending to increase this deflection. This term could also be evaluated numerically, but the following argument suggests that it can be simply omitted.

Consider a membrane whose planform has a typical scale c and which is divided into N elements. A typical element then

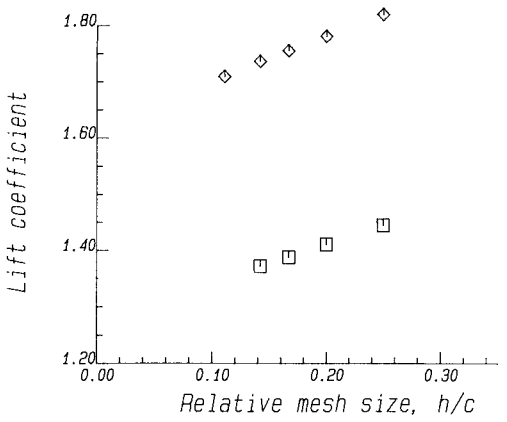

Fig. 4 Dependence of lift coefficient on element size (◇, rigid surface; □, elastic surface).

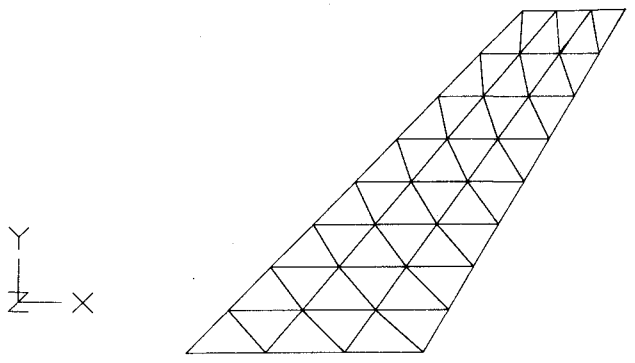

Fig. 5 Paneling for a swept wing.

has a scale of $h = c/\sqrt{N}$, thickness d, and elastic modulus E. If one node is displaced normal to the surface by an infinitesimal amount ϵh, then potential theory suggests that the change in pressure force will be of order $q\epsilon h^2$. The restoring elastic forces will be much smaller because the strain is of order ϵ^2. However, if the node is given an in-plane displacement of the same amount, the aerodynamic change is negligible, whereas the restoring elastic force will be around ϵEdh. Thus an overall measure of the relative importance of elastic and aerodynamic terms in the Jacobian is given by the ratio of these two restoring forces, $Ed/qh = AE\sqrt{N}$, giving a physical significance to the aeroelastic number AE defined previously. In a typical application we could have $Ed = 3MN/M$, $q = 100$ Pa, and $c = 10$ m, giving $AE = 3000$. As N is also at least 20, the aerodynamic term clearly contributes only a very small part to the stiffness. An exception to this occurs for cambered wings at less than design incidence. The stagnation point then moves to the top surface, causing a local inversion of camber (called luffing). As the initial cambered shape has nearly zero stiffness to pressure forces directed toward the center of curvature, convergence difficulties may be expected unless the aerodynamic stiffness is known.

This concludes the description of the method. Considerable improvements in speed can be obtained with careful attention to the way in which the stiffness and influence matrices are calculated, and also by assembling these only when necessary.

III. Numerical Results

Accuracy and Convergence

In order to determine the dependence of the solution of the number of elements used to model a wing, tests were run

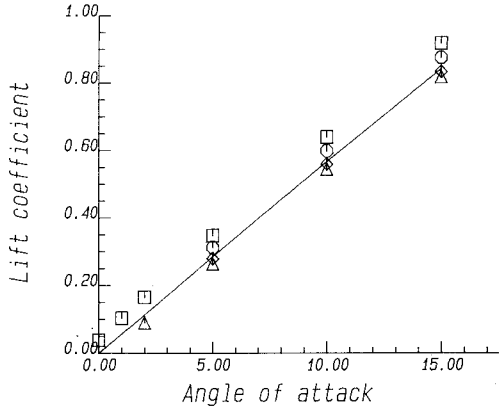

Fig. 6 Lift coefficient of swept wing, for different boundary conditions and membrane elasticity (——, rigid surface; restrained trailing edge: ◯, $AE = 10^4$; □, $AE = 10^3$; free trailing edge ◇, $AE = 10^4$; △, $AE = 10^3$).

on a triangular sail-like shape. The semispan wing planform and a sample mesh are shown in Fig. 1. Increases in mesh size were carried out keeping the number of subdivisions of the base chord and semispan equal, thus retaining the regular mesh configuraton. The membrane was completely restrained along the leading edge and at the clew (point B), and the root chord AB was a line of symmetry. The wing was set at angle of attack of 20 deg, and the membrane material modeled as a linear isotropic sheet with no initial twist or camber and an aeroelastic number AE of 10^3.

The results for the lateral displacement of the trailing edge are shown in Fig. 2. The number of mesh points has very little effect on this shape—the agreement is excellent. However, because the membrane has a relatively high elastic stiffness and small curvature, small changes in shape lead to rather larger changes in membrane forces, so edge restraint forces and membrane stresses show a greater dependence on mesh size. Figure 3 shows the x component of the (nondimensional) force required to restrain the wing at point B when the wing pressure is fixed at a uniform value ($c_p = 1.0$), so that the accuracy is governed by the finite-element procedure only. It can be seen to be proportional to $N^{-1/2}$ (that is, to a typical element dimension, h/c) as expected for a formulation using N constant-strain elements.[22] This figure also shows the force required when the pressure is calculated using the vortex-lattice method; the accuracy is less good for a given N, but still depends on $N^{-1/2}$. The vortex-lattice itself can be tested by restraining the entire wing surface. This gave the lift coefficient shown in Fig. 4, where once again the $N^{-1/2}$ dependence is evident. The two parts of the solution procedure are therefore consistent in their order of accuracy of nodal forces.

The classical quadrilateral vortex lattice is known to converge as $1/N$, so the present layout is relatively inefficient. This is because the method is sensitive mostly to the number of spanwise partitions, but here the chordwise partitions are being multiplied at the same rate to maintain the uniform and regular mesh. As noted previously, better results can be expected by a little experimentation with the lattice configuration, and indeed the same is true for the finite-element method. It might prove difficult to find meshes which benefit both parts of the solution, but it seems likely that increasing the element density in corners and toward the wingtips would help.

Convergence of the iteration procedure used to obtain each particular solution is governed primarily by the Newton-Raphson method and the extent to which the initial membrane shape is in equilibrium with its pressure distribution. The convergence rate is quadratic once the iteration

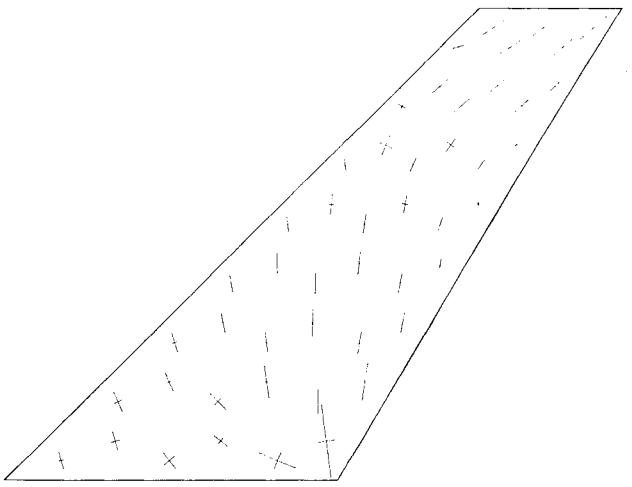

Fig. 7 Stress distribution with unrestrained trailing edge.

comes within the radius of convergence. Highly cambered shapes generally have a high geometric stiffness and converge within 7 or 8 iterations, but cases in which the pressure loading causes large shape changes may take 20 or more iterations. The presence of stress singularities in the corners also affects convergence, and restraining a few extra corner nodes speeds the solution greatly.

Example

In order to demonstrate some of the effects of membrane stretch on aerodynamics, some results are given for the semiplanform shown in Fig. 5. The membrane is fixed at least along the leading edge and wing tip, and the root chord is a line of symmetry with the trailing-edge point also fixed. The wing is initially uncambered and untwisted.

The lift coefficient vs angle of attack obtained for the corresponding rigid wing using the same mesh is shown in Fig. 6. For small angles of attack the lift slope is 0.0572, whereas Lamar[23] gives 0.0583 for a 3×15 quadrilateral lattice on the same planform. If the membrane is now allowed to stretch but is restrained round all its edges, the stretch causes camber to develop and thus increases the lift, as also shown in Fig. 6. This increase is most marked at small angles of attack since at higher angles the acquired camber gives the membrane some geometric stiffness which makes it much more resistant to further increases in load. An interesting effect occurs at zero incidence where the wing apparently self-inflates, developing camber which is held in place by the resulting pressure difference across the surface. This effect is also predicted for two-dimensional sails, and since the stresses for this set of boundary conditions run predominantly in the chordwise direction it is not surprising to see it occur here.

When the trailing edge is released the wing develops twist which now reduces the lift, as shown by Fig. 6. There is still some induced camber, and whether or not the lift is greater or less than that for the rigid surface depends on the planform shape and the nature of the edge restraints—in this case the twist dominates and the wing develops less and less lift as the stretch increases (that is, as AE decreases). Solutions could not be obtained for small angles of incidence. This is probably because the twist then causes leading parts of the wing to incur pressure loading in the opposite direction (backwinding), leading to convergence problems for the reasons given earlier.

The distribution of membrane stress for this final case is shown in Fig. 7. Here the line segments are proportional to the principal stresses and lie in the same directions. It can be seen that many of the elements do not exhibit a second principal stress, which means that the membrane is wrinkled there (or just about to wrinkle). This behavior has been observed in other problems studied using this method, particularly those regarding triangular sail shapes.[14] The wrinkling is simply caused by the highly nonuniform loading applied by the edge restraints, which in turn is caused by the absence of restraints on the trailing edge. A simple demonstration of this is easily made by stretching a handkerchief between two points, and a simple theoretical example can be found in Timoshenko and Goodier[24] where nonuniform tensile forces applied to the ends of a thin strip are shown to lead to a region of transverse compression in the center of the strip. The theory of wrinkled membranes originated with Kondo et al.,[25] although their results have been rediscovered several times since. The results are that the stress field is nondivergent, and that the wrinkle lines run along the geodesics of the surface. These conditions would greatly simplify an analytic approach to the current problem, if only it was known a priori that the whole surface was wrinkled when under load.

IV. Conclusions

The method outlined in this paper solves for the final shape and stresses of membrane wings under aerodynamic loading. As far as the authors are aware, this has not been previously possible for three-dimensional wings of arbitrary shape. While neither the finite-element nor the vortex-lattice methods are new, the novel part of this work lies in the combination of the two. It has been shown that the two methods are consistent in their order of accuracy, and that the iteration method employed is almost always convergent.

The procedure has numerous applications. Besides the more obvious aerodynamic problems of hang-gliders and parawings, its general potential lies in the study of yacht sails. As the finite-element model can also include beam elements, it is now possible to analyze the structural and aerodynamic performance of complete yacht rigs or of aircraft that incorporate membranes as lifting surfaces.

References

[1]Thwaites, B., "Aerodynamic Theory of Sails—Part I," *Proceedings of the Royal Society*, A261, 1961, pp. 402–422.

[2]Nielsen, J. N., "Theory of Flexible Aerodynamic Surfaces," *Journal of Applied Mechanics*, Vol. 30, 1968, pp. 435–442.

[3]Newman, B. G., "The Aerodynamics of Flexible Membranes," *Proceedings of the 8th Canadian Congress of Applied Mechanics*, University of Moncton, New Brunswick, Canada, 1982, pp. 63–78.

[4]Nielsen, J. N., Kriebel, A. R., Goodwin, F. K., Barakat, B., Rudin, M., and Burrell, J. A., "Theoretical Aerodynamics of Flexible Wings at Low Speeds—I, One-lobed Parawings," Vidya Rept. 84, 1963.

[5]Sneyd, A. D., Bundock, M. S., and Reid, R., "Possible Effects of Wing Flexibility on the Aerodynamics of Pteranodon," *The American Naturalist*, Vol. 120, 1982, pp. 455–477.

[6]Ormiston, R. A., "Theoretical and Experimental Aerodynamics of the Sailwing," *Journal of Aircraft*, Vol. 8, 1971, pp. 77–84.

[7]Holla, V. S., Roa, K. P., Asthana, C. B., and Arokkiaswamy, A., "Aerodynamic Characteristics of Pretensioned Elastic Membrane Rectangular Sailwings," *Computer Methods in Applied Mechanics & Engineering*, Vol. 44, 1984, pp. 1–16.

[8]Milgram, J. H., "The Analytical Design of Yacht Sails," *Transactions of SNAME*, Vol. 76, 1968, pp. 118–160.

[9]Milgram, J. H., "Sail Force Coefficients for Systematic Rig Variations," *SNAME Technical & Research Rept. R-10*, 1971.

[10]Thrasher, D. F., Mook, D. T., and Nayfeh, A. H., "A Computer-Based Method for Analyzing the Flow Over Sails," *Chesapeake Sailing Yacht Symposium*, SNAME, Annapolis, MD, 1983, pp. 119–127.

[11]Register, D. S., "Analysis of Steady Flow Over Interacting Sails," Ph.D. Thesis, University of Florida, Gainesville, 1981.
[12]Jackson, P. S., "A 3.D Aeroelastic Sail Model," *Proceedings of Science of Sail Design*, Boundary Layer Wind Tunnel Lab., University of Western Ontario, Canada, 1972, pp. 55–68.
[13]Christie, G. W., "Analysis of the Mechanics of Bioprosthetic Heart Valves," Ph.D. Thesis, Dept. of Theoretical & Applied Mechanics, University of Auckland, New Zealand, 1982.
[14]Jackson, P. S., "The Analysis of Three-Dimensional Sails," *Proceedings of the 10th Canadian Congress of Applied Mechanics*, University of Western Ontario, London, Canada, 1985, pp. 59–67.
[15]Oden, J. T. and Sato, T., "Finite Strains and Displacements of Elastic Membranes by the Finite Element Method," *International Journal of Solids Structures*, Vol. 3, 1967, pp. 471–488.
[16]Hearman, R., *An Introduction to Applied Anisotropic Elasticity*, Oxford Univ. Press, London, 1961.
[17]Fung, Y. C., *Foundations of Solid Mechanics*, Prentice-Hall, NJ, 1965.
[18]James, R. M., "On the Remarkable Accuracy of the Vortex Lattice Method," *Computational Methods in Applied Mechanics & Engineering*, Vol. 1, 1972, pp. 55–79.
[19]Asfar, K. R., Mook, D. T., and Nayfeh, A. H., "Application of the Vortex Lattice Technique to Arbitrary Bodies," *Journal of Aircraft*, Vol. 16, 1979, pp. 421–424.
[20]Newman, B. G. and Goland, H. T., "Two Dimensional Inflated Buildings in a Cross Wind," *Journal of Fluid Mechanics*, Vol. 117, 1982, pp. 507–530.
[21]Margason, R. J. and Lamar, J. E., "Vortex-Lattice FORTRAN Program for Estimating Subsonic Aerodynamic Characteristics of Complex Planforms," NASA TN D-6142, 1971.
[22]Strang, G. and Fix, G. F., *An Analysis of the Finite Element Method*, Prentice-Hall, NJ, 1973.
[23]Lamar, J. E., "A Modified Multhopp Approach for Predicting Lifting Pressures and Camber Shape for Composite Planforms in Subsonic Flow," NASA TN D-4427, 1968.
[24]Timoshenko, S. and Goodier, N., *Theory of Elasticity*, McGraw-Hill, New York, 2nd ed., 1951.
[25]Kondo, K., Iai, T., Moriguti, S., and Murasaki, T., "Tension-Field Theory," *Memoirs of the Unifying Study of the Basic Problems in Engineering Sciences by Means of Geometry*, Vol. 1, Gakajutsu Buinmken Fukyu-kai, Tokyo, 1955, pp. 61–85.